

- and the program was switched to an identical profile incorporating an elevated annealing temperature of 54°C and was repeated 35 times. The amplification product was digested with the enzymes Pst I and Sal I and purified from an agarose gel with the glassmilk resin supplied in the GeneClean kit. The plasmid containing the mature toxin was digested with the same enzymes to create a vector for directional cloning. Subclones were screened by DNA sequencing. The GenBank accession number for the gene encoding IVB and IVC is U15925.
13. D. Phillips, N. A. Saccomano, R. A. Volkman, U.S. Patent 5,122,596 (1992).
 14. The sequence and primary activity of IVB and IVC are available (13) [M. E. Adams *et al.*, *Mol. Pharmacol.* **44**, 681 (1993); T. Teramoto *et al.*, *Biochem. Biophys. Res. Commun.* **196**, 134 (1993)]. The presence of two toxins with identical primary structures was reported more recently [A. H. Ganong *et al.*, *Soc. Neurosci. Abstr.* **19**, 7212 (1993)].
 15. A library of all diastereomers was synthesized to verify that the chromatography used to distinguish the native proteolytic fragments could resolve all possible isomers of this peptide. The proteolytic products Gly-Leu-LSer-Phe-Ala and Gly-Leu-DSer-Phe-Ala from native venom each independently coeluted with one of the synthesized peptide diastereomers (7).
 16. Peptide synthesis was done on an ABI 430A (Applied Biosystems, Foster City, CA) with the use of *tert*-butoxycarbonyl protocols (version 1.4; 1-methyl-2-pyrrolidinone and hydroxybenzotriazole). Capping was done after each coupling step. Butoxycarbonyl (BOC) AlaPAM (0.66 g, 0.753 mmol/g) resin and standard side-chain-protected BOC amino acids were used in chain assembly. Hydrofluoric acid (HF) deprotection and cleavage from resin (500 mg) followed the low-high method of J. Tam and colleagues [*J. Am. Chem. Soc.* **105**, 6442 (1983)]. The crude HF product (262 mg) was stirred into 1 liter of 0.4% trifluoroacetic acid (TFA) for 1 hour, then pH-adjusted to 8.0 with NH₄OH and filtered with a 0.22- μ m filter. The solution was swirled once daily. Reversed-phase HPLC showed that a major product developed in 8 to 12 days. Active toxin was purified from the refolding by means of reversed-phase chromatography on a POROS R2M column (25.4 \times 100 mm) by ion exchange on a polysulfoethylsartamide column (4.6 \times 200 mm), and by rpHPLC on a C-18 Vydac column (4.6 \times 250 mm). Synthetic IVB and IVC were shown to be identical to the corresponding native toxins in all respects.
 17. Chromatography was done as a C-18 Vydac column (4.6 \times 250 mm), with a particle size of 5 μ m and a pore size of 300 Å. Flow rate was 1 ml/min; detection occurred at 220 nm. The gradient was A = 0.1% TFA, B = acetonitrile. The concentration of B was 25 to 35% over 40 min, then 35% for 10 min. Results obtained were identical to those outlined in Fig. 1, A through C.
 18. Animals used in these studies were treated in strict accordance with the *NIH Guide for the Care and Use of Laboratory Animals* (NIH Publ. no. 85-23, U.S. Department of Health and Human Services, Public Health Department, Bethesda, MD, 1985). Freshly dissociated cerebellar Purkinje neurons from rats 7 to 15 days postnatal were prepared by means of a modification of described methods [L. J. Regan, *J. Neurosci.* **11**, 2259 (1991); J. E. Huettner and R. W. Baughman, *ibid.* **6**, 3044 (1986)]. Whole-cell recordings of P-type currents (carried by Ba²⁺) were recorded at room temperature with 1- to 3-megohm patch electrodes containing 90 mM CsOMs, 18 mM CsF, 9 mM EGTA, 9 mM Hepes, 4 mM MgCl₂, 14 mM creatine phosphate (2 Na), 1 mM tris-guanosine triphosphate, and 4 mM Mg-adenosine triphosphate, adjusted to pH 7.3 with CsOH and to 325 mosM with sucrose. The extracellular buffer for seal formation contained 150 mM NaCl, 10 mM Hepes, 4 mM KCl, 2 mM CaCl₂, 3 mM BaCl₂, 2 mM MgCl₂, and 10 mM deoxyglucose at pH 7.4. After a seal was obtained and whole-cell recording was done, the extracellular medium was switched to 154 mM tetraethylammonium chloride, 10 mM Hepes, 5 mM BaCl₂, 2 mM MgCl₂, 10 mM deoxyglucose, and 0.25 mM tetrodotoxin, adjusted to pH 7.4 and to 335 mosM. Series resistance was compensated by 80%.

- Cells were voltage-clamped at -80 mV, and maximum inward barium currents were induced by a 50-ms depolarizing step to -10 to +10 mV. Leak current was subtracted with four scaled hyperpolarizing pulses stepped from a holding potential of -80 mV. Test solutions were delivered through 152- μ m microcapillary tubes by gravity feed. Toxin peptide solutions contained cytochrome c (1 mg/ml). Currents recorded under these conditions were blocked 95 \pm 1% ($n = 8$) by 200 nM synthetic IVA and were blocked 6 \pm 1% ($n = 9$) by a combination of 3.2 μ M ω -conotoxin GVIA and 10 μ M nifedipine.
19. S. D. Heck *et al.*, data not shown.
 20. ⁴⁵Ca²⁺ flux into rat brain synaptosomes was done essentially as described in (5). Synaptosomes were preincubated with toxin for 30 min (20 min at 4°C and 10 min at 30°C) before depolarization with 45 mM KCl in the presence of 0.5 μ Ci of ⁴⁵Ca²⁺. The ⁴⁵Ca²⁺ flux was 0.053 \pm 0.015 nmol per milligram of protein. Each concentration data point represents the mean \pm SEM for at least three determinations except where noted.
 21. Partial sequence data has been reported [fraction M in (7)].
 22. Venom (~100 μ l) was diluted with PBS (100 μ l), loaded on a G-75sf gel column (10 mm inside diameter \times 10 cm), and eluted with PBS at 400 μ l/min, collecting 1.4-ml fractions.
 23. Electrospray mass spectrometry data was collected as described in (7).
 24. The COOH-terminal five-amino acid peptides of IVB and IVC (Gly-Leu-DLSer-Phe-Ala) were used as model substrates to study the proteolytic activity in fractions 3 and 4. The COOH-terminal five-amino acid peptide of IVB, containing a D-serine residue, was completely resistant to proteolysis and retarded the cleavage of the analogous L-amino acid substrate derived from IVC. The protease was isolated from venom and shows a high homology to neutral endopeptidase class 24.11 (lanes 3 and 4, Fig. 4). Alignment with related proteases places residue 1 of

- this enzyme with residue 53 of homologs. The extremely hydrophobic NH₂-terminus in the later enzymes is suggested to serve as a membrane anchor. The spider protease lacking this element may be designed as a soluble protein either for injection into prey or to serve as a necessary protease for toxin selection or maturation.
25. Gel fractions 9, 10, and 11 were combined, lyophilized, and reconstituted in 500 μ l of water. To 200 μ l of this sample was added 20 μ l of 50 mM EDTA and 20 μ g of IVC or IVB as a solution in 20 μ l of water. The sample was kept at 37°C for the duration of the experiment.
 26. K. Richter, R. Egger, G. Kreil, *Science* **238**, 200 (1987).
 27. G. Kreil, *J. Biol. Chem.* **269**, 10967 (1994).
 28. T. Yamauchi *et al.*, *ibid.* **267**, 18361 (1992); G. Rudnick and R. H. Abeles, *Biochemistry* **14**, 4515 (1975).
 29. K. A. Gallo and J. R. Knowles, *Biochemistry* **32**, 3981 (1993); K. A. Gallo, M. E. Tanner, J. R. Knowles, *ibid.*, p. 3991; M. E. Tanner, K. A. Gallo, J. R. Knowles, *ibid.*, p. 3998.
 30. C. Walsh, *Enzymatic Reaction Mechanisms* (Freeman, San Francisco, CA, 1979), pp. 828-834.
 31. N. S. Lamango and R. E. Isaac, *Insect Biochem. Mol. Biol.* **23**, 801 (1993).
 32. U. Hornberg, N. T. Davis, J. G. Hildebrand, *J. Comp. Neurol.* **303**, 35 (1991); L. Schoohfs, S. Schrooten, R. Huybrechts, A. DeLoof, *Gen. Comp. Endocrinol.* **69**, 1 (1988).
 33. R. Ford *et al.*, *Comp. Biochem. Physiol. C* **85**, 61 (1986).
 34. M. Grabner *et al.*, *FEBS Lett.* **339**, 189 (1994). See (4) for mammalian channel cloning.
 35. The authors acknowledge the contributing efforts of L. H. Hirring, A. M. Mueller, L. D. Artman, J. L. Ives, J. A. Lowe, E. F. Nemeth, K. F. Geoghegan, G. O. Daumy, T. J. Carty, J. G. Stroh, C. Drong, K. Rosnack, and F. Fuller.

27 June 1994; accepted 5 October 1994

Spermine and Spermidine as Gating Molecules for Inward Rectifier K⁺ Channels

Eckhard Ficker, Maurizio Tagliatela, Barbara A. Wible, Charles M. Henley, Arthur M. Brown*

Inward rectifier K⁺ channels pass prominent inward currents, while outward currents are largely blocked. The inward rectification is due to block by intracellular Mg²⁺ and a Mg²⁺-independent process described as intrinsic gating. The rapid loss of gating upon patch excision suggests that cytoplasmic factors participate in gating. "Intrinsic" gating can be restored in excised patches by nanomolar concentrations of two naturally occurring polyamines, spermine and spermidine. Spermine and spermidine may function as physiological blockers of inward rectifier K⁺ channels and "intrinsic" gating may largely reflect voltage-dependent block by these cations.

Gating of voltage-dependent ion channels is generally thought to be an intrinsic property of the channel protein (1). However,

E. Ficker and B. A. Wible, Department of Molecular Physiology and Biophysics, Baylor College of Medicine, One Baylor Plaza, Houston, TX 77030, USA.

M. Tagliatela, Department of Neurosciences—Section of Pharmacology, Second School of Medicine, University of Naples "Federico II," 5 Via S. Pansini, 80121 Naples, Italy.

C. M. Henley, Department of Otorhinolaryngology, Baylor College of Medicine, One Baylor Plaza, Houston, TX 77030, USA.

A. M. Brown, Rammelkamp Center, Metro Health System, and Department of Physiology, Case Western Reserve University, Cleveland, OH 44109-1998, USA.

*To whom correspondence should be addressed.

gating may be specifically modified by accessory proteins (β subunits) (2), small organic molecules (for example, adenosine triphosphate) (3), or inorganic cations such as Ca²⁺ or Mg²⁺ (4-6). The intrinsic gating of inward rectifier K⁺ channels (IRKs) (6, 7) is thought to contribute to inward rectification by producing closure of channels at depolarized potentials, resulting in negligible outward currents even in the absence of intracellular Mg²⁺ (Mg_i²⁺). Conversely, reopening of channels at hyperpolarized potentials is thought to cause the time-dependent onset of inward currents. Two IRKs, IRK1 (8) and ROMK1 (9), ex-

pressed heterologously in *Xenopus* oocytes, differ in both rectification (10) and gating (11) phenotypes. Currents from IRK1 exhibit time dependence upon activation and rectify strongly, whereas onset of the weakly rectifying ROMK1 currents is virtually instantaneous. A single negatively charged residue (Asp¹⁷² in IRK1) in putative transmembrane domain M₂ appears to be critically involved in time-dependent gating (11, 12).

Cytoplasmic factors might also be involved in the time dependence of IRK currents (6, 13). In cell-attached macropatches from *Xenopus* oocytes, IRK1 inward currents activated with marked time dependence and the rates were voltage-dependent, becoming faster at more hyperpolarized potentials (14). When patches were excised in the inside-out configuration in the absence of Mg²⁺, transient outward currents appeared at depolarized potentials (Fig. 1A). The decay of the outward current became progressively slower with time and could not be restored upon patch exposure to Mg²⁺ (Fig. 1C). Likewise, time dependence of inward currents disappeared (Fig. 1A, inset). However, time dependence was recovered if the patch was brought near the oocyte (Fig. 1B), suggesting that a particle unrelated to Mg²⁺ has been washed away.

Because the key gating determinant (Asp¹⁷² in IRK1) is negatively charged (11), we postulated that small, positively charged intracellular molecules might control or influence the gating of IRK1. Therefore, we tested the three naturally occurring polyamines (PAs)—spermine (SPM), spermidine (SPD), and putrescine (PUT)—for their ability to restore time dependence to IRK1 currents. The internal application of all three PAs to excised, inside-out patches resulted in a block of outward currents in IRK1 (Fig. 1D). Only SPM and SPD, however, were able to produce time-dependent block (Fig. 1E). SPM and SPD act as high-affinity blockers, since only nanomolar concentrations were required to mimic the time dependence of IRK1 currents. By contrast, the block by PUT was time-independent and required concentrations a 1000-fold higher than for SPM and SPD (15).

Consistent with time-dependent block, the current decay was faster with increasing SPM and SPD concentrations (Fig. 1F). The block was also voltage-dependent, becoming more marked at more depolarized potentials. At the single channel level, SPM and SPD shortened openings and markedly prolonged closures (Fig. 1G), thereby producing the observed decay in the ensemble currents (Fig. 1E and 1F).

We tested the importance of the Asp residue at position 172 (11, 12) for block by SPM or SPD. Asp¹⁷² was critical for SPM and SPD effects, since no detectable time-

Table 1. PAs in *Xenopus* oocytes and in K⁺-Ringer solution-bathing oocytes. Total PA levels were measured from single *Xenopus* oocytes according to established procedures (18, 19). Molar concentrations were calculated assuming a volume of 1 μl per oocyte (n = 3, mean ± SD). To estimate PA levels outside oocytes, five groups of 10 oocytes each were incubated in 100 or 500 μl of K⁺-Ringer. After 15 min, the bathing solution was aspirated and frozen for analysis (n = 8, mean ± SD).

Polyamines	<i>Xenopus</i> oocyte		Bathing solution
	Polyamines (pM/μg protein)	Polyamines (μM)	Polyamines (μM)
SPM	0.88 ± 0.02	216.51 ± 19.94	0.076 ± 0.15
SPD	3.35 ± 0.19	824.53 ± 85.73	0.34 ± 0.28
PUT	3.53 ± 0.31	869.42 ± 85.89	1.35 ± 1.29

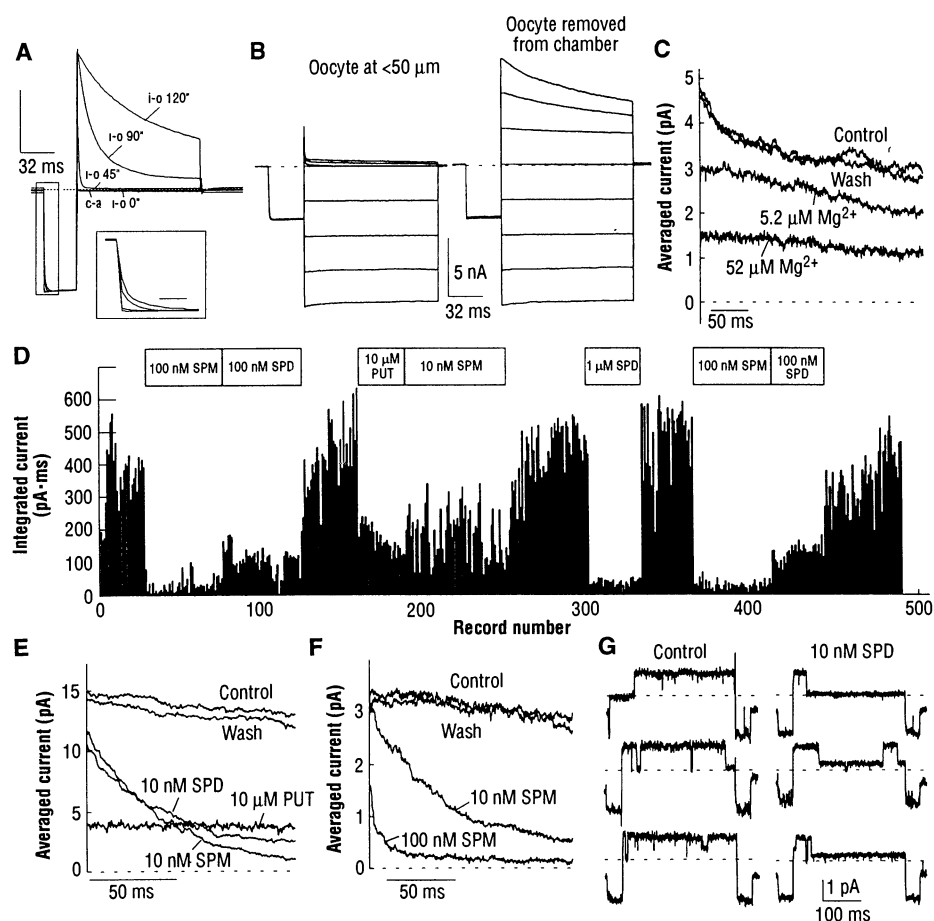


Fig. 1. Loss of IRK1 gating and restoration by SPM and SPD. (A) Uncorrected cell-attached (c-a) and inside-out (i-o) macropatch recordings from *Xenopus* oocytes injected with IRK1 complementary RNA. The records were taken at the indicated times after patch excision. Holding potential, 0 mV; prepulse to -30 mV; test pulse, +40 mV. The records were normalized at the steady-state current level at -30 mV. The vertical scale bar was 3 nA for the i-o 90-s (90°) trace, 1.41 nA for the c-a trace, 2.58 nA for the i-o 0° trace, 2.96 nA for the i-o 45° trace and 2.92 nA for the i-o 120° trace. Inset, expanded scale (2-ms bar) of time-dependent inward currents. (B) The time-dependent component is restored when the patch is positioned within 50 μm of the oocyte. Holding potential, 0 mV; prepulse to -30 mV, test pulses from -80 mV to +60 mV in 20-mV steps. (C) Ensemble average of 16 to 48 single channel records, recorded in control solution after exposure of i-o patch to 5.2 and 52 μM Mg²⁺ and upon washout. Test potential: +40 mV. As judged from the peak current, the patch contained five to eight channels. (D) Integrated single channel outward currents from a multichannel (three to five IRK1 channels) patch in the i-o configuration, exposed to the indicated concentrations of PAs for the indicated times. Traces were recorded with 3-s intervals. Test potential, +40 mV; test pulse duration, 150 ms. (E and F) Ensemble average of 16 to 48 single channel records from multichannel patches [20 to 25 channels in (E); 4 to 6 in (F)] recorded in the i-o configuration in control solution and upon exposure to the indicated concentrations of PAs. Test potential, +40 mV. (G) Single channels recorded in the i-o configuration in control solution and upon exposure to 10 nM internal SPD. Test potential, +40 mV. Pre- and post-pulses, -80 mV. Dashed lines indicate zero current.

dependent block of IRK1 D172N was elicited (Fig. 2, B and C). Moreover, higher concentrations were required to produce the time-independent block (Fig. 2, A and D), with SPM and SPD block more affected than block by PUT. The dissociation constant (K_d) values for SPM, SPD, and PUT block at +40 mV were calculated from averaged single channel currents: 7.5 ± 1 nM ($n = 9$), 17.9 ± 3.3 nM ($n = 11$), and 9800 ± 2300 nM ($n = 5$), respectively, in IRK1, while in D172N they were 258 ($n = 2$), 446 ± 172 ($n = 3$), and $26,700 \pm 6300$ ($n = 4$), respectively. Single channel recordings from D172N showed that the blocked state produced by SPM and SPD had a much shorter lifetime than in IRK1 (compare Fig. 2E and Fig. 1G) and that frequent reopenings resulted in sustained ensemble currents (Fig. 2, B and C). PUT showed even faster blocking rates that were comparable in both wild-type and D172N channels.

The key role of the Asp for the time-dependent gating produced by SPM and SPD was also tested in ROMK1. This channel has an Asn at the corresponding residue, rectifies weakly, and lacks time-dependent activation (9, 11). Substitution with an Asp (N171D) resulted in strong rectification and prominent time dependence of inward and outward macropatch currents (11, 16), which were lost after excision (Fig. 3A). As for IRK1, reconstitution of time-dependent behavior could be achieved by positioning the macropatch in close proximity to the oocyte (Fig. 3B). Internal application of SPD (1 and 3 μ M) reproduced the time-dependent block induced by approaching the oocyte (Fig. 3C). Single channel currents showed that SPD shortened open times and increased closed times (Fig. 3D), consistent with the slow open-channel block observed in IRK1 channels. By contrast, block of wild-type ROMK1 channels required much higher SPM and SPD concentrations and did not exhibit any time dependence (Fig. 3, E and F). The key role of the Asp is further emphasized by the 10^4 -fold difference in K_d values for SPD block between ROMK1 and ROMK1 N171D. The values calculated from macropatch currents at +40 mV were 303.5 nM for ROMK1 N171D ($n = 29$) and 2.16 mM for ROMK1 ($n = 16$). Just as with IRK1, PUT was unable to confer rectification and time-dependent activation to ROMK1 N171D.

The specificity of SPM and SPD was further confirmed by testing other small positively charged molecules for their effects on ROMK1 N171D. We tested a variety of diamines including 1,3-diaminopropane, 1,6-diaminohexane, 1,7-diaminohexane, and 1,8-diaminooctane, and they all blocked ROMK1 N171D in a manner sim-

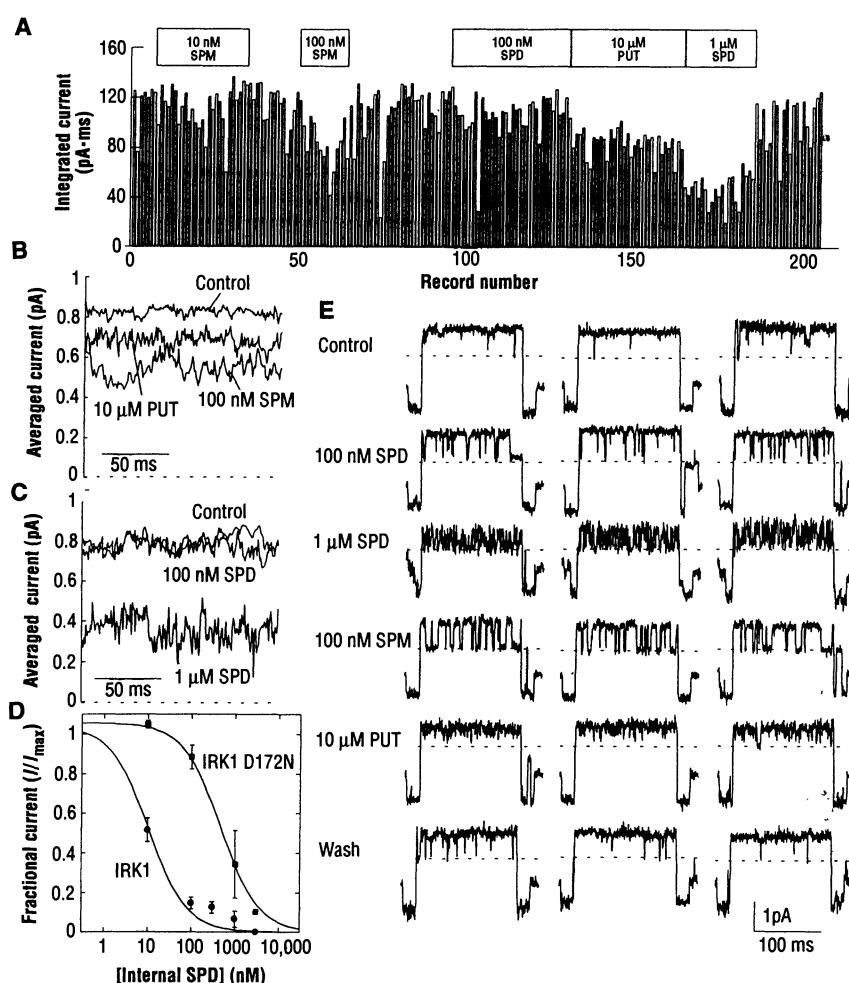


Fig. 2. Loss of time-dependent block by SPM and SPD in IRK1 D172N mutant channels. **(A)** Integrated single channel outward currents from a patch containing a single IRK1 D172N channel in the i-o configuration, exposed to the indicated concentrations of PAs for the indicated times. Traces were recorded with 3-s intervals. Test potential, +40 mV; Test pulse duration, 150 ms. **(B and C)** Averaged IRK1 D172N single channel records (16 to 48 records) recorded in i-o configuration in control solution and upon exposure to the indicated concentrations of PAs. Test potential, +40 mV. **(D)** Dose-response for blockade by SPD in IRK1 and IRK1 D172N channels. The single channel current from 16 to 64 sweeps for each SPD concentration was integrated (I) and the normalized values (I/I_{max}) were expressed as a function of the intracellular SPD concentration. Solid lines are fits to the following binding isotherm: $y = \max/(1 + X/K_d)^n$, where X is the SPD concentrations and n the Hill coefficient. Fitted values for n were between 0.8 and 1.2. In the displayed fits, n was fixed at 1. **(E)** Single channels recorded from IRK1 D172N channels expressed in *Xenopus* oocytes in the i-o configuration in control solution, after subsequent exposure to 100 nM SPD, 1 μ M SPD, 100 nM SPM, 10 μ M PUT, and upon washout. Test potential, +40 mV; pre- and post-pulses, -80 mV. Dashed lines indicate zero current.

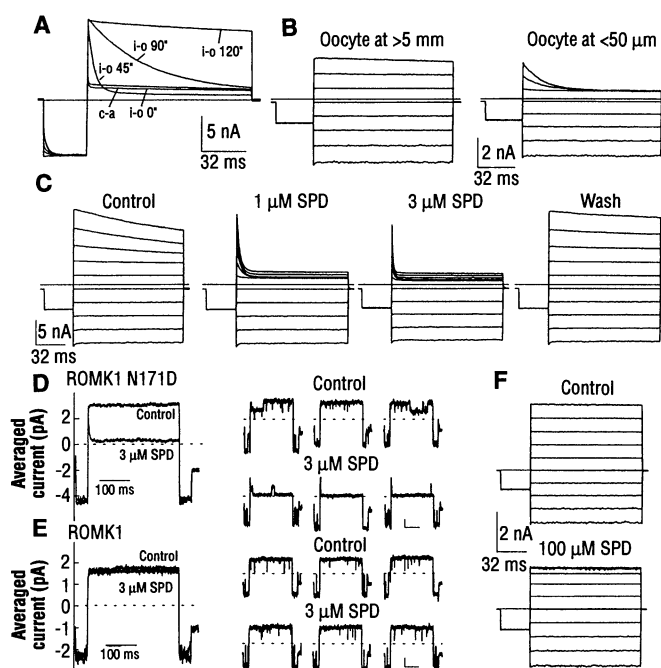
ilar to PUT but not SPM or SPD.

SPD is also responsible for the time dependence of inward currents, illustrated for ROMK1 N171D (Fig. 4). Similar results were obtained with SPM. Thus, the origin of the time dependence of both inward and outward currents is related; for inward currents, block by SPM/SPD is being relieved while for outward currents it is being initiated. After complete loss of time dependence after patch excision in Mg_i^{2+} -free solution (Fig. 4B), 10 μ M SPD reconstituted the time dependence of inward currents displayed by N171D in the cell-attached macropatch (Fig. 4, C and E). SPD also strongly blocked the outward currents, pro-

ducing a transient relaxation. Simultaneous addition of 0.5 mM free Mg_i^{2+} , together with 10 μ M SPD, slowed the relaxation at +40 mV (Fig. 4D). Similar to results described for IRK1 channels, less influence was exerted by Mg_i^{2+} on the kinetics of inward current activation in ROMK1 N171D. These observations are compatible with a competitive interaction between the two cations and are consistent with the eightfold increase in the affinity for Mg_i^{2+} in ROMK1 N171D (11, 16).

To test further the role of PAs as physiological regulators of IRKs, we have measured total SPM, SPD, and PUT concentrations in *Xenopus* oocytes (Table 1). These

Fig. 3. Comparison of SPD effects on ROMK1 and ROMK1 N171D channels. **(A)** Unsubtracted c-a and i-o macropatch recordings from *Xenopus* oocytes injected with ROMK1 N171D cRNA. The records were taken at the indicated times after patch excision. Holding potential, 0 mV; prepulse to -30 mV; test pulse, $+40$ mV. Dashed line indicates zero current. The records were normalized as described in Fig. 1A. The vertical scale bar was 5 nA for the i-o 90° and i-o 120° traces, 3.09 nA for the c-a trace, 4.55 nA for the i-o 0° trace, and 4.95 nA for the i-o 45° trace. **(B)** The time-dependent component in ROMK1 N171D channels is restored when the patch is positioned within $50 \mu\text{m}$ from the oocyte. Holding potential, 0 mV; prepulse to -30 mV; test pulses from -80 mV to $+60$ mV in 20-mV steps. **(C)** Effect of 1 and $3 \mu\text{M}$ SPD on ROMK1 N171D currents. Holding potential, 0 mV; prepulse to -30 mV; test pulses from -80 mV to $+100$ mV in 20-mV steps. **(D)** Averaged and single channel traces of ROMK1 N171D recorded in control solution and after patch exposure to $3 \mu\text{M}$ SPD. Test potential, $+40$ mV; pre- and post-test pulses to -80 mV. The patch contained two channels. Scale bars correspond to 1 pA and 100 ms. **(E)** Averaged and single channel traces of wild-type ROMK1, recorded in control solution and after patch exposure to $3 \mu\text{M}$ SPD. Test potential, $+40$ mV; pre- and post-test pulses to -80 mV. The patch contained one channel. Scale bars, 1 pA and 100 ms. **(F)** Effects of $100 \mu\text{M}$ SPD on wild-type ROMK1 macropatch currents. Holding potential, 0 mV; prepulse to -30 mV; test pulses from -80 mV to $+100$ mV in 20-mV steps. Solid or dashed lines indicate zero current.



lar determinants for Mg_i^{2+} binding and K^+ conduction in IRK1 (10). It appears that the mechanism of inward rectification involves a fast, voltage-dependent, time-independent block by Mg_i^{2+} together with a slower, voltage- and time-dependent block, probably exerted by SPM and SPD. In IRK1 these processes seem to be largely separable; block by Mg_i^{2+} has been localized mainly to the carboxyl terminus (10), whereas time-dependent gating is conferred by the Asp in the M_2 region (11, 12). SPM and SPD may be the physiological molecules responsible for time-dependent "intrinsic" gating and the Asp in M_2 may contribute to the receptor site for SPM and SPD. It remains to be determined whether the kinetics of IRK currents are influenced by the physiological fluctuations in SPM and SPD that occur during cell growth and division (17).

REFERENCES AND NOTES

- B. Hille, *Ionic Channels of Excitable Membranes* (Sinauer, Sunderland, MA, ed. 2, 1992).
- L. I. Isom, K. S. DeJongh, W. A. Catterall, *Neuron* **12**, 1183 (1994).
- S. J. H. Ashcroft and F. M. Ashcroft, *Cell. Signal.* **2**, 197 (1990).
- A. L. Blatz and K. L. Magleby, *Trends Neurosci.* **10**, 463 (1987); H. Matsuda, A. Saigusa, I. Irisawa, *Nature* **325**, 156 (1987); C. A. Vandenberg, *Proc. Natl. Acad. Sci. U.S.A.* **84**, 2560 (1987).
- R. D. Harvey and R. E. Ten Eick, *J. Gen. Physiol.* **91**, 593 (1988); R. A. Aldrich, *Nature* **362**, 107 (1993); Y. Shimoni, R. B. Clark, W. R. Giles, *J. Physiol. (London)* **448**, 709 (1992); J. M. B. Anumwo, L. C. Freeman, W. M. Kwok, R. S. Kass, *Cardiovasc. Drug Rev.* **9**, 299 (1991).
- H. Matsuda, *J. Physiol. (London)* **397**, 237 (1988).
- K. Ishihara, T. Mitsuye, A. Noma, M. Takano, *ibid.* **419**, 297 (1989); M. R. Silver and T. E. DeCoursey, *J. Gen. Physiol.* **96**, 109 (1990); P. R. Stanfield *et al.*, *J. Physiol. (London)* **475**, 1 (1994).
- Y. Kubo, T. Baldwin, Y. N. Jan, L. Y. Jan, *Nature* **362**, 127 (1993).
- K. Ho *et al.*, *ibid.* **362**, 31 (1993).
- M. Taglialatela, B. A. Wible, R. Caporaso, A. M. Brown, *Science* **264**, 844 (1994).
- B. A. Wible, M. Taglialatela, E. Ficker, A. M. Brown, *Nature* **371**, 246 (1994).
- P. R. Stanfield *et al.*, *J. Physiol. (London)* **478**, 1 (1994).
- A. N. Lopatin, E. N. Makhina, C. G. Nichols, *ibid.* **477**, 86P (1994).
- Mutagenesis of IRK1 and ROMK1 as well as heterologous expression of their complementary RNAs in *Xenopus* oocytes was as described [B. A. Wible, M. Taglialatela, E. Ficker, A. M. Brown, *Nature* **371**, 246 (1994)]. In both single channel and macropatch recordings [D. W. Hilgemann, *Pfluegers Arch.* **415**, 247 (1989)], the pipette solution was K^+ -Ringer (100 mM KCl, 2 mM MgCl_2 , 10 mM Hepes, pH 7.3), while the bath solution was iso- K^+ (100 mM KCl, 10 mM EDTA, and 10 mM Hepes, pH 7.3). MgCl_2 was added to bath solutions in which 10 mM EDTA was substituted for EGTA to achieve free Mg^{2+} concentrations of 5.2 and $52 \mu\text{M}$ [A. Fabiato and F. Fabiato, *J. Physiol. (Paris)* **75**, 463 (1979)]. Macropatch data were filtered at 3 to 8 kHz and digitized at 10 to 33 kHz, and single channel data were filtered at 1 kHz and digitized at 5 to 10 kHz. SPM, SPD, and PUT were from Sigma (St. Louis, MO).
- IRKs are not the only ion channels affected by PAs. Calcium channels [R. H. Scott, K. G. Sutton, A. C. Dolphin, *Trends Neurosci.* **16**, 153 (1993)], calcium-activated K^+ channels [T. Weiger and A. J. Hermann, *J. Membrane Biol.* **140**, 133 (1994)], and

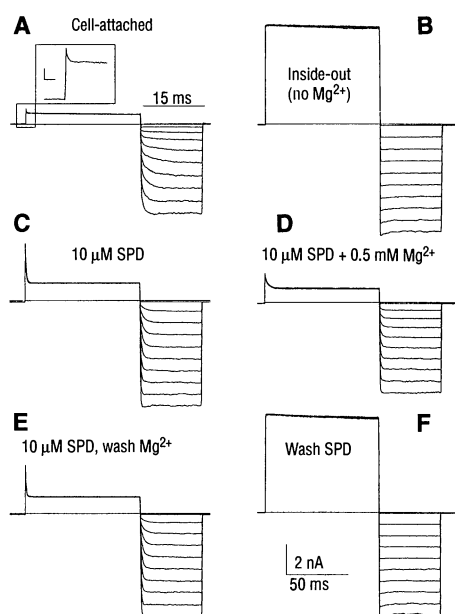


Fig. 4. Effect of Mg_i^{2+} on SPD-induced blockade of ROMK1 N171D channels. After recording from a cell-attached macropatch showing time-dependent inward and outward (see inset A; bars are 200 pA and 2 ms) currents **(A)**, the patch was excised in Mg_i^{2+} -free solution and the time dependence of the currents was lost **(B)**. Subsequently, the intracellular side of the patch was exposed to $10 \mu\text{M}$ SPD **(C)**, $10 \mu\text{M}$ SPD plus 0.5 mM free Mg_i^{2+} **(D)**, and again to $10 \mu\text{M}$ SPD **(E)**. **(F)** Traces recorded after SPD washout. In all panels, the holding potential was 0 mV; depolarizing prepulse to $+40$ mV; and test pulse from 0 mV to -45 mV in -5 -mV steps. Solid lines indicate zero current.

cised patches in close proximity to an oocyte. The results are also consistent with the observation that cells have specific membrane systems for transporting PAs (17).

The effects of SPM and SPD on IRK1, IRK1 D172N, ROMK1, and ROMK1 N171D channels confirm that time-dependent gating is due to interaction with the Asp. However, the time-independent component of SPM and SPD block was still much stronger in IRK1 D172N than in wild-type ROMK1, suggesting that additional sites might contribute to the block of IRK1. These sites may be located in the carboxyl terminus, which specifies molecu-

concentrations are compatible with a role for PAs as IRK blockers. Furthermore, PAs could be detected in the K^+ -Ringer solution-bathing *Xenopus* oocytes (Table 1) and could account for the restoration of time-dependent gating after positioning ex-

glutamate receptors [P. N. R. Usherwood and I. S. Blagbrough, *Pharmacol. Therap.* **52**, 245 (1992); K. Williams, C. Romano, M. C. Dichter, P. B. Molinoff, *Life Sci.* **48**, 469 (1991)] are also blocked by PAs, although at much higher concentrations (at least 10^3 -fold) than those required for IRKs. External application of PAs had no effects on IRK1 currents.

16. Z. Lu and R. MacKinnon, *Nature* **371**, 243 (1994).
17. A. E. Pegg, *Cancer Res.* **48**, 759 (1988).
18. N. D. Brown, M. P. Strickler, J. M. Whaun, *J. Chromatogr.* **245**, 101 (1982).
19. M. Brock and C. M. Henley, *Hear. Res.* **72**, 37 (1994).
20. We thank L. Jan for providing the IRK1 clone; W.-Q. Dong, D. Jackson, and R. Cockrell for injecting

and handling oocytes; and T. Affini, C. Zhu, and S. Dou for expert molecular biology support. Supported in part by NIH grants NS23877, HL36930 (A.M.B.), HL37044 (B.A.W.), DC00656 (C.M.H.), Texas Heart Association grant 94G218 (M.T.), and a grant from A. von Humboldt Foundation (E.F.).

8 October 1994; accepted 27 October 1994

TECHNICAL COMMENTS

Stellar Variability and Global Warming

Stellar observations (1, 2) suggest that the sun is less variable in its total light output than other stars of comparable magnetic activity. In his report (3), Peter Foukal offers an interpretation of this result in terms of a model for solar variability. It appears, however, that this model does not account completely and correctly for the stellar observations.

Foukal argues that the broadband variability of a star like the sun is explainable in terms of two types of discrete magnetic features on its surface, namely bright faculae (in both active regions and the magnetic network) and dark sunspots. A central feature of his interpretation of the stellar observations is the expectation that the variation in total light must be dominated by the dark (spot) component when the average activity exceeds some level.

This model can, indeed, explain the high amplitude brightness variability of stars that are considerably younger than the sun. Such stars have time-averaged magnetic activity several times greater than that of the present-day sun. Their total light output also characteristically varies inversely with their emission in the resonance lines of ionized calcium (widely accepted as a proxy for the bright faculae), a fact implying that their net broadband variability is driven by the dark (that is, spot) component, consistent with Foukal's expectation.

Stars similar in age to the sun, however, have time-averaged magnetic activity comparable to that of the present-day sun (4). They show calcium emission variations on the time scale of the 11-year solar activity cycle ranging from about one-half to twice that of the corresponding solar variation. Their broadband variability ranges from 0.1%, which is characteristic of the sun, to values as much as ten times larger. The broadband cyclic variation of the sun seems to be a factor of 3 or 4 below what one would expect for a star with this average magnetic activity, despite the fact that the amplitude of the sun's calcium emission variation appears to be fairly typical.

These stars, including the sun, character-

istically share a property that clearly distinguishes them from younger stars: Their total light output varies directly with their calcium emission, rather than inversely. In terms of the two-component model, this means that, regardless of its amplitude, the net broadband variability of these stars is dominated by the bright (facular) component. Thus, Foukal's argument that the dark (spot) component is driving the net broadband variability of some of these stars (the more strongly varying, in particular) is not correct. Accordingly, his interpretation does not explain, in a fundamental, qualitative way, the behavior of those stars he is most concerned with, namely, stars with average magnetic activity comparable to that of the present sun, but with broadband variability amplitudes that are several times larger.

Furthermore, the behavior of some of these solar analogs appears to pose quantitative difficulties for the two-component model of solar and stellar variability itself. Consider, for example, the star HD 10476. Its average magnetic activity is only 6% greater than that of the sun. The decadal variation of its calcium emission, however, exceeds that from the sun by a factor of almost two. If the proportionality between calcium emission and the bright (facular) component is similar for both the sun and its stellar analogs (5), then the contribution to HD 10476's broadband variation from the bright component must also be about twice the corresponding solar value, or 0.4%. Photometric measurements show that its net broadband variation, which reflects the contribution from the dark as well as the bright component, is about 0.6%, six times the solar value. In conjunction, these two measured relations imply that the "dark" component must make a positive contribution of 0.2% to the decadal variation of this star, which is, of course, contradictory.

In total, somewhat more than one-third (5 of 13) of the observed sample of close solar analogs pose similar difficulties. If we include stars that are clearly less active than the sun, the situation remains about the

same: 8 of 21 stars in the augmented sample are discordant. Perhaps solar-stellar variability does involve "other mechanisms than modulation by photospheric magnetism . . ." (3, p. 239). For example, there may be some large-scale phenomenon going on that is not accounted for by a two-component model that views variability as the sum of contributions from small-scale features alone (6).

In any case, it seems evident that such problems in explaining the behavior of solar analog stars must also cast doubt on conclusions about the range of possible solar variability and the consequent implications for studies of global warming. I disagree with the suggestion that the observation of relatively large amplitude variability among sun-like stars is not particularly relevant to "the explanation or prediction of Earth's climate anomalies in the immediate past or future" (3, p. 238). Were the sun simply to regress to the mean defined by its stellar analogs, it would experience variations in its total light output several times larger than those measured during the past 15 years, without any accompanying change in its average magnetic activity. Until we have a consistent explanation for the observed behavior of solar analog stars, it would seem imprudent to dismiss the clues that stellar observations are providing us about the range of possible solar behavior.

Richard R. Radick
Air Force Phillips Laboratory,
Solar Research Branch,
Post Office Box 62,
Sunspot, NM 88349, USA

REFERENCES AND NOTES

1. R. R. Radick, G. W. Lockwood, S. L. Baliunas, *Science* **247**, 39 (1990).
2. G. W. Lockwood, B. A. Skiff, S. L. Baliunas, R. R. Radick, *Nature* **360**, 653 (1992).
3. P. Foukal, *Science* **264**, 238 (1994).
4. A. Skumanich, *Astrophys. J.* **171**, 565 (1972).
5. The existence of a tight empirical relationship between calcium emission and stellar rotation rate, the former an end consequence of stellar magnetic activity and the latter a property that is generally believed to be causally linked to its generation through a dynamo mechanism, offers evidence that this proportionality does not vary widely from star to star. [See, for example, R. W. Noyes, L. W. Hartmann, S. L. Baliunas, D. K. Duncan, A. H. Vaughan, *Astrophys. J.* **279**, 763 (1984)].
6. One possibility is discussed in [J. R. Kuhn, K. G. Libbrecht, R. H. Dicke, *Science* **242**, 908 (1988); J. R. Kuhn and K. G. Libbrecht, *Astrophys. J.* **381**, L35 (1991)].

30 June 1994; accepted 8 September 1994